Chemical Shielding Anisotropy of Protonated and Deprotonated Carboxylates in Amino Acids

Zhengtian Gu and Ann McDermott*

Contribution from the Department of Chemistry, Columbia University, New York, New York 10027

Received October 13, 1992

Abstract: The carbon chemical shielding of carboxylate groups in microcrystalline amino acids has been measured and correlated with the protonation state. As had been observed in solution NMR studies, there is a small but reproducible change in the isotropic chemical shift upon protonation for any given amino acid with a magnitude of -4 ± 2 ppm; however, the environmentally-induced shifts and generally poor resolution in solid-state spectra would prevent interpretation of such a small shift in typical applications. More interestingly, the anisotropy as manifested in the shape of the envelope of sideband intensities for low speed spinning spectra is obviously different for protonated and deprotonated salts even without data fitting. In particular, σ_{11} and σ_{22} exhibit large changes upon protonation: σ_{22} changes from 177 ± 10 to 155 ± 20 while σ_{11} changes from 242 ± 4 to 257 ± 4. It is known that the most shielded element of the tensor, σ_{33}, is perpendicular to this plane, and this element is independent of protonation state, with a value of 110 ± 6 for deprotonated and 110 ± 4 for protonated compounds. These changes in σ_{11} and σ_{22} are opposite in sign and approximately compensate or cancel in their contributions to the average shift, $\sigma_{iso} = {}^1/_3(\sigma_{11} + \sigma_{22} + \sigma_{33})$. On the other hand, various measures of the asymmetry of the tensor accentuate these changes. These functions provide reliable criteria for the protonation state; for example $A = \sigma_{11} + \sigma_{33} - \sigma_{22}$ changes from 173 ± 12 to 211 ± 20 upon protonation. For both the carboxylic acids and the carboxylates there is a wide range of values for σ_{22}; we have not yet satisfactorily analyzed the origins of this variation although they probably include hydrogen bonding effects.

Introduction

Methods for the assignment of charges and hydrogen bonding environments for ionizable amino acid side groups in proteins, particularly the carboxylates, are typically indirect and difficult. A case of great interest is the membrane-associated "proton pumps", including the photosynthetic reaction centers, bacteriorhodopsin (bR) and ATP synthetase. Invariably a crucial role has been convincingly established in their mechanisms for carboxylate side groups by means of mutational analysis or chemical modification studies, while the other ionizable side groups have been proposed as participants in some studies. Elucidation of a mechanism for proton transfer reactions in solids and membrane proteins requires spectroscopic fingerprinting of the protonation state and hydrogen bonding environment of these groups, and particularly for the carboxylates. FTIR spectroscopy is a viable approach for analyses of the protonation states of carboxylates and has been extensively used for bR[1] and also for the photosynthetic reaction centers.[2] As an alternative method, carbon NMR spectra and the correlation of proton resonances to the carbon signals might be assigned by simple strategies by virtue of selective ^{13}C labeling. An ongoing effort to analyze the solid-state NMR spectra of aspartic acids in bR has been reported.[3]

Previous work on ^{13}C spectra of carboxylic acids in aqueous solution shows a small increase in shielding (ca. 3 ppm) upon protonation.[4] For solid-state studies this magnitude of shift is difficult to analyze reliably and we have pursued the information in the anisotropies instead. The orientations and values of the shielding tensors have been assigned for several deprotonated carboxylates in amino acids[5] and various protonated and deprotonated oxalic acid salts.[6] These studies have been reviewed[7] and generally support a distinct change in the orientations of the tensors as a function of formal protonation state: the most shielded element, σ_{33}, is consistently orthogonal to the plane of the heavy atoms, and the least shielded direction is along the C–C bond (or the bisector of the O–C–O angle) for deprotonated groups, while it is orthogonal to the carbonyl for protonated groups. In contrast to this very careful work on the orientations of these tensors, we could not find an adequate database for the values of these tensors

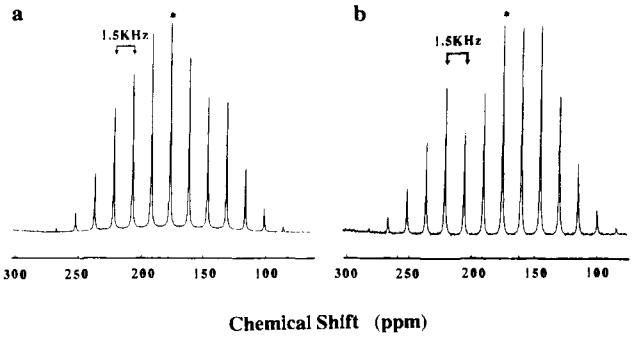

Figure 1. Low speed spectra of (1-^{13}C)glycine, an example of a deprotonated carboxy group (a), and (4-^{13}C)aspartic acid, a protonated carboxy group (b). The spectra are plotted together with the corresponding simulations and illustrate the clear differences in the sideband patterns. The asterisks identify centerband peaks, and the arrows below the spectra indicate spinning speeds, which dictate the spacings of the sidebands.

(1) (a) Rothschild, K.; He, Y.; Sonar, S.; Marti, T.; Khorana, H. G. *J. Biol. Chem.* **1992**, *267*, 1615–1622. (b) Eisenstein, L.; Lin, S.; Dollinger, G.; Odashima, K.; Termini, J.; Konno, K.; Ding, W.; Nakanishi, K. *J. Am. Chem. Soc.* **1987**, *109*, 6860–6862. (c) Ormos, P.; Chu, K.; Mourant *J. Biochem.* **1992**, *31*, 6933–6937. (d) Braiman, M.; Mogi, T.; Marti, T.; Stern, L.; Khorana, H.; Rothschild, K. *Biochemistry* **1988**, *27*, 8516–8520. (e) Dollinger, G.; Eisenstein, L.; Lin, S.; Nakanishi, K.; Odashima, K.; Termini, J. *Methods Enzymol.* **1986**, *127*, 649–662.

(2) Hienerwadel, R.; Thibodeau, D.; Lenz, F.; Nabedryk, E.; Breton, J.; Kreutz, W.; Mäntele, W. *Biochemistry* **1992**, *31*, 5799–5808.

(3) (a) Engelhard, M.; Hess, B.; Emeis, D.; Metz, G.; Kreutz, W.; Siebert, F. *Biochemistry* **1989**, *28*, 3967–3975. (b) Metz, G.; Siebert, F.; Engelhard, M. *Biochemistry* **1992**, *31*, 455–462.

(4) (a) Surprenant, H.; Sarneski, J.; Key, R.; Byrd, J.; Reilly, C. J. *Magn. Reson.* **1980**, *40*, 231–243. (b) Rabenstein, D.; Sayer, T. *J. Magn. Reson.* **1976**, *24*, 27–39.

(5) (a) Naito, A.; Ganapathy, S.; Akasaka, K.; McDowell, C. *J. Chem. Phys.* **1981**, *74*, 3190–3197. (b) Haberkorn, R.; Stark, R.; van Willigen, H.; Griffin, R. *J. Am. Chem. Soc.* **1981**, *103*, 2534–2539. (c) James, N.; Ganapathy, S.; Oldfield, E. *J. Magn. Reson.* **1983**, *54*, 111–121.

(6) Griffin, R.; Pines, A.; Pausak, S.; Waugh, J. *J. Chem. Phys.* **1975**, *63*, 1267–1271.

(7) Veeman, W. *Prog. NMR Spectrosc.* **1984**, *16*, 193–235.

0002-7863/93/1515-4282$04.00/0

Table I. Tensor Elements of Carboxyl Groups in Amino Acids

		σ_{11}	σ_{22}	σ_{33}	σ_{iso}	ρ	A
1	alanine[a]	240	184	110	178	–0.13	166
2	arginine	233	180	107	173	–0.15	160
3	asparagine	243	170	108	174	0.08	181
4	aspartic (DL)	243	176	107	175	–0.01	174
5	aspartic (L)	242	179	106	176	–0.07	169
6	cysteine	239	173	109	174	0.01	175
7	cystine	243	174	108	175	0.01	177
8	glutamine	241	172	106	173	0.02	175
9	glutamatic	243	185	107	179	–0.15	165
10	glycine	241	178	111	177	–0.04	174
11	isoleucine	243	175	108	175	0.01	176
12	leucine	242	180	108	177	–0.07	170
13	lysine	242	179	109	177	–0.05	172
14	methionine	240	182	109	177	–0.11	167
15	proline	238	173	113	175	0.04	178
16	serine	242	174	111	175	0.04	179
17	sodium aspartate (DL)[b]	243	185	107	178	–0.15	165
18	sodium glutamate	239	200	107	182	–0.42	146
19	sodium glutamate (δ)	242	202	105	183	–0.42	145
20	threonine	243	168	107	172	0.11	182
21	valine	245	176	106	175	–0.01	175
	deprotonated groups[c]	242 ± 4	177 ± 10	110 ± 6	175 ± 4	–0.02 ± 0.14	173 ± 12
22	alanine hydrochloride	254	163	111	176	0.28	202
23	aspartic (DL γ)	260	166	107	178	0.24	201
24	aspartic (L γ)	254	163	107	175	0.25	199
25	aspartic hydrochloride (DL)	257	148	107	171	0.43	212
26	aspartic hydrochloride (DL γ)	260	157	107	174	0.35	210
27	glutamatic (δ)	259	173	110	180	0.15	196
28	glutamatic hydrochloride	256	165	107	176	0.23	198
29	glycine hydrochloride	254	155	111	173	0.39	210
30	isoleucine hydrochloride	255	147	111	171	0.50	219
31	leucine hydrochloride	257	153	109	173	0.41	213
32	lysine dihydrochloride	254	148	112	171	0.49	218
33	methyl leucine ester	258	151	111	173	0.46	218
34	methyl serine ester	257	138	113	170	0.65	232
35	valine hydrochloride	257	148	110	172	0.49	219
	protonated groups[c]	257 ± 4	155 ± 20	110 ± 4	174 ± 6	0.38 ± 0.28	211 ± 20

[a] Unless otherwise indicated we refer to the C-1 (backbone) carboxyl carbon of the L amino acid. $\rho \equiv (\sigma_{11} + \sigma_{33} - 2\sigma_{22})/(\sigma_{11} - \sigma_{33})$; $A \equiv \sigma_{11} - \sigma_{22} + \sigma_{33}$. [b] The two carboxylates were unresolved. [c] Average ±2 standard deviations, excluding methyl esters and sodium salts.

as a function of protonation state, especially for the case of amino acids in typical hydrogen bonding environments. Veeman's review on carbon tensor analyses concludes the discussion of carboxylates with the speculation that there may be no general rule for decoding the protonation state from a chemical shielding analysis. We report here a systematic study of the magic angle spinning spectra of amino acids in which the protonation state of the carboxylate group was deliberately changed by variation in the crystallization conditions, attempting to emphasize those salts that have a published crystal structure. For the more restrictive database of carboxylates in amino acids, we found a simple rule for determination of protonation states.

Materials and Methods

The amino acids were purchased from Sigma Chemical Co. and were recrystallized from water. The HCl salts were crystallized from 20–25% HCl solution and the NaOH salts were prepared by addition of 2 equiv of sodium hydroxide to an aqueous solution. The methyl esters were recrystallized from methanol water mixtures. (4-^{13}C)Aspartic acid was synthesized as previously described[1c] and (1-^{13}C)glycine was purchased from Cambridge Isotope Laboratories (Cambridge, MA).

All spectra were taken on a Chemagnetics CMX400 operating at 99.71 MHz for ^{13}C and 396.5 for ^{1}H. A standard cross polarization pulse sequence with the usual phase cycling was used, with a contact time of 3 ms, a 4.5 μs 90° pulse for protons, and acquisition times of 25 ms. Generally a recycle delay of 3 s was used and 600 to 12000 transients were accumulated. All spectra were recorded at room temperature and referenced using adamantane (run separately).

The principal values of the chemical shift tensors were extracted by computer simulation of the spectrum using the algorithm developed by Herzfeld and Berger and a minimization routine based on the CERN-Minuit programs.[8] We attempted to assign error bars based on repetition of certain experiments at different speeds.

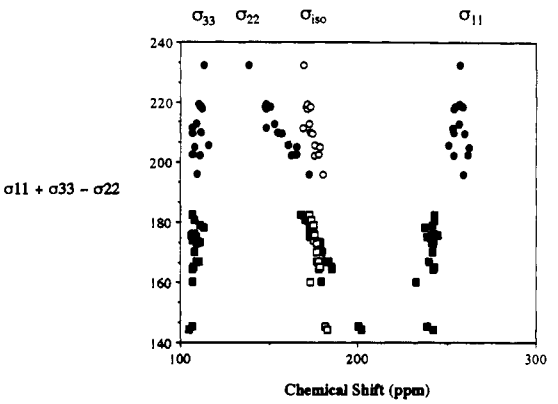

Figure 2. The three tensor elements (solid symbols) and the isotropic shift, $\sigma_{iso} = {}^1/_3(\sigma_{11} + \sigma_{22} + \sigma_{33})$ (open symbols) are plotted for all amino acids in the survey as a function of the asymmetry $A = \sigma_{11} + \sigma_{33} - \sigma_{22}$. According to the typical convention. the elements are labeled as follows: 110 ppm, σ_{33}; 150–200 ppm, σ_{22}; and 220–270 ppm, σ_{11}. The squares represent deprotonated carboxylates, and the circles are protonated carboxylic acids or esters.

Results

Typical low-speed MASS spectra for a protonated (4-^{13}C)-aspartic acid) and a deprotonated ((1-^{13}C)glycine) carboxy group

(8) deGroot, H.; Harbison, G.; Herzfeld, J.; Griffin, R. *Biochemistry* **1989**, *28*, 3346–3353.

Table II. Protonation-Induced Shifts of Tensor Elements of Carboxylates

		$\Delta\sigma_{11}$	$\Delta\sigma_{22}$	$\Delta\sigma_{33}$	$\Delta\sigma_{iso}$	$\Delta\rho^a$	ΔA^a
1	Ala·HCl/Ala	14	−21	0	−2	0.41	36
2	Asp·HCl/Asp	14	−28	0	−6	0.44	42
3	Glu·HCl/Glu	13	−20	0	−3	0.38	33
4	Gly·HCl/Gly	13	−24	0	−4	0.43	36
5	Ile·HCl/Ile	12	−28	3	−4	0.49	43
6	Leu·HCl/Leu	15	−27	1	−4	0.49	43
7	Lys·HCl/Lys	12	−31	3	−6	0.54	41
8	Val·HCl/Val	12	−28	4	−3	0.48	44
average shift[b]		13 ± 1	−26 ± 3	1 ± 2	−4 ± 1	0.46 ± 0.04	40 ± 3

[a] $\rho \equiv (\sigma_{11} + \sigma_{33} - 2\sigma_{22})/(\sigma_{11} - \sigma_{33})$; $A \equiv \sigma_{11} - \sigma_{22} + \sigma_{33}$. [b] Average ±2 standard deviations, excluding methyl esters and sodium salts.

are shown in Figure 1, with centerbands marked with asterisks. These data illustrate the prominent change in sideband pattern that we observed. We simulated spectra of a variety of natural abundance amino acids to obtain the principle elements of the shielding tensors. The tensor elements for the ^{13}C spectra of all the amino acids are tabulated in Table I.

Figure 2 displays the tensor elements for all of the compounds as a function of an asymmetry function, $A = \sigma_{11} + \sigma_{33} - \sigma_{22}$. (We note that the general observations reported in this paper would still be valid if the more frequently used asymmetry parameters, $\sigma_{11} - {}^1/_2(\sigma_{22} + 2\sigma_{33})$, $\rho = (\sigma_{11} + \sigma_{33} - 2\sigma_{22})/(\sigma_{11} - \sigma_{33})$, or $\sigma_{11} - \sigma_{22}$, were used instead, but in the final analysis A provided a statistically more significant measure for separating the carboxylates according to chemical environment so we utilize this function throughout.) This figure illustrates the range in values for all three tensor elements for protonated and deprotonated groups, and the ordinate serves simply to spread out the values for visualization. Examination of the dependence of each of the tensor elements shows that σ_{33} and σ_{iso} are essentially invariant, but σ_{11} and σ_{22} both have large variations, shifting in opposing senses upon protonation. The variation in σ_{11} is essentially bimodal, depending principally on protonation state as illustrated by the average values in Table I. The variation in σ_{22} is not bimodal, but for each protonation state it shows a dependence on some other factors such as the nature or conformation of the side group or the hydrogen bonding environment. These protonation-induced changes in σ_{11} and σ_{22} nearly cancel in the calculation of σ_{iso} while the anisotropy functions have the effect of accentuating these opposite variations in σ_{11} and σ_{22}.

We collected in Table II the changes upon protonation for each of the tensor elements and the anisotropy for every pair of compounds; for example, we subtracted parameters for glycine from those for the HCl salt of glycine. This table illustrates that, although there is a large spread in the values for σ_{22} among deprotonated and protonated groups, the *shifts* in σ_{iso}, σ_{11}, and σ_{22} upon protonation are remarkably constant. This result is suggestive of a group additivity effect of the side chain. Therefore we studied the chemical shielding of aspartic acid in a variety of protonated and deprotonated compounds (unpublished). All of these spectra followed our rule for determining protonation states from the shielding anisotropy. Surprisingly, for this collection of aspartic acid complexes we also observed a broad range of values for σ_{22} so we cannot ascribe this variability to the side chain structure alone.

Discussion

For carboxy groups in amino acids the change in protonation state causes an unmistakable and reliable change in tensor anisotropy. Conversely, we can assign a protonation state for a carboxy group based solely on the CSA analysis. We are encouraged by the fact that the sideband intensity differences are obvious even before curve fitting analyses and that this analysis is feasible for low-sensitivity samples.

The zwitterionic (deprotonated) forms of alanine, threonine, and glycine have been previously analyzed by single-crystal methods,[5] and our values for the tensor elements agree well with those determinations. The data reported previously on bacteriorhodopsin[3] and Asp-containing model compounds (with the exception of the C-terminal residue from bacteriorhodopsin) generally give unambiguous protonation states from an analysis based on A, ρ, or $\sigma_{11} - \sigma_{22}$, and these assignments agree in every case with the protonation assignments proposed by Metz et al.

Earlier work on carboxylates, which embraced a wider variety of compounds than simply amino acids, indicated a variability in tensor values for each protonation state that was larger than that observed in this survey. For some of those salts, the inability to identify the protonation state clearly by tensor analysis might result from important variability in the internal electronic structure; for example, for the oxalates the conformation may affect the degree of conjugation in the molecule.

The trends in the specific values of the three tensor elements described in the results section are interesting in light of the known spatial assignments for these tensor elements. For example σ_{33}, which is orthogonal to the plane of the heavy atoms, shows no notable dependence on protonation state or on amino acid side group. σ_{11} is probably along the C—C vector for deprotonated salts and is orthogonal to the C=O double bond for protonated salts and was systematically less shielded for deprotonated as compared with protonated groups. σ_{22}, which is probably along the C=O double bond for protonated salts and orthogonal to the C—C vector for deprotonated salts, shows a consistent increase in shielding upon protonation. Unlike the other two elements it also shows a substantial variation in values for either protonated or deprotonated groups. In the following we discuss the possible reasons for this variation in σ_{22} or A. We have not yet attempted a calculation of the shielding anisotropy which would surely be helpful in understanding the trends.

To assess the sensitivity of the anisotropy to the chemical environment, we divided the data into five classes of carboxyl groups based on the chemical form of the amino acid: (1) methyl esters, (2) HCl (protonated) carboxylate salts of the backbone carboxy group, (3) aspartate and glutamate side chains that are protonated in the solid state, (4) deprotonated carboxylates in the zwitterionic salts of amino acids, and (5) sodium salts of aspartate and glutamate side chains. This series relates approximately to the expected electron density for the $CO_2\cdots X$ bonds ($X = Na, H, CH_3$). In Figure 3 we display the full range observed for the isotropic shift (left) and the asymmetry function (right) for each group. The protonated Asp and Glu side chains give values for A comparable to those for the HCl salts of the backbone carboxyl carbons. It is of particular interest that the sodium salts gave a substantially different range in values for A as compared with those for the zwitterionic compounds. This observation and the large difference between protonated and deprotonated groups caused us to consider whether A might therefore serve also as an approximate indicator of hydrogen bonding strength, *within* the protonated or deprotonated salts.

It is of note that proton spectra of the HCl salts and the protonated side chain of Asp taken by means of combined rotation and multiple pulse (CRAMPS) methods exhibited proton chem-

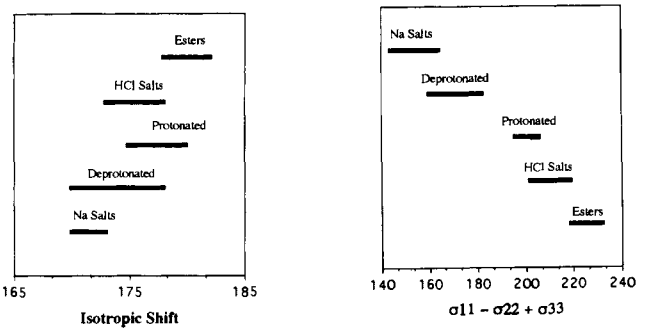

Figure 3. The full ranges of observed values for the parameter $A = \sigma_{11} + \sigma_{33} - \sigma_{22}$ and the isotropic shifts $\sigma_{iso} = {}^1/_3(\sigma_{11} + \sigma_{22} + \sigma_{33})$ are displayed. The compounds are organized in terms of five categories: (1) methyl esters, (2) protonated HCl salts of the backbone carboxy group, (3) protonated aspartate and glutamate side chains, (4) deprotonated carboxylates in the zwitterionic salts of amino acids, and (5) sodium salts of aspartate and glutamate side chains. The methyl esters were represented by only two compounds, protonated side groups by five compounds, sodium salts by three compounds. HCl salts by eight compounds, and deprotonated (zwitterionic) by eightteen compounds.

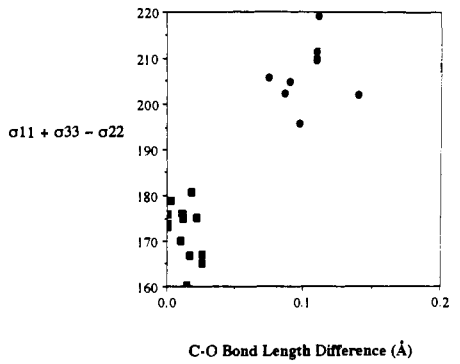

Figure 4. The parameter $A = \sigma_{11} + \sigma_{33} - \sigma_{22}$ is plotted as a function of the difference in C–O bond lengths for each compound for which we could find previously reported X-ray or neutron diffraction structures; this databank includes most of the zwitterionic and HCl salts but not the esters or the Na salts. The distribution of the compounds in terms of asymmetry of the tensor is bimodal and divides the compounds exactly into deprotonated (squares) and protonated (circles) compounds.

ical shifts for the carboxylic acid group that varied only from 11.0 to 11.3 ppm, with line widths of approximately 2 ppm (McDermott, unpublished). Thus, to our surprise, the proton shielding appears to be insensitive to the hydrogen bonding variation in these compounds, and it does not correlate with the carbon anisotropy.

Most of the zwitterionic amino acids and the HCl salts utilized in this study have published X-ray and neutron diffraction structures (although the sodium salts and methyl esters do not). Within the category of HCl salts of carboxylic acids, or of zwitterions, we tested whether variations in the shielding tensor elements correlate with any structural parameters. A typical structural indication for protonation state in a carboxy group is the difference in C–O bond lengths. Figure 4 displays the correlation between the difference in C–O bond lengths in the carboxy group and the function A. We observed perfectly correlated bimodal distributions for both parameters, such that the protonated and deprotonated forms fall into distinct classes. Within each class, protonated or deprotonated, there is a wide range of observed values for A and for the bond length difference, but the correlation between the two characteristics is quite poor. It is not obvious that the difference in C–O bond lengths is the best metric for hydrogen bonding. However, neither does A correlate systematically with O–H bond lengths (which were available for a smaller set of compounds by virtue of neutron diffraction results) nor with O···N hydrogen bonding distances (although in many cases it is apparent that there are multiple hydrogen bond partners for each oxygen so it was not obvious how to analyze the network of comparable hydrogen bond distances).

In contrast, recently reported work on carbonyls in hydrogen bonded amides[9] indicated a nice correlation between the O···N distance and the σ_{22} element of the ^{13}C chemical shielding tensor. One important difference between these two studies is that the databank for the study of amide carbonyls was from a limited number of compounds in which the same amino acid was in different peptide environments but approximately the same geometry and moreover one predominant hydrogen bonding partner could be identified. These authors point out that alanine and glycine, for example, give very different functional dependences of the shift tensor elements on hydrogen bond length. Similarly, our work indicated that the variation in σ_{22} partly reflects the nature of the side chain; Table II illustrates that the protonation-induced shift in σ_{22} is a rather fixed number whereas the range of σ_{22} for various protonated or various deprotonated compounds is much larger. In order to study whether hydrogen bond environment also contributes to the value for σ_{22} and more importantly whether something can be learned about the hydrogen bonding environment from measuring σ_{22}, we are now embarking on an extensive study of the aspartate and glutamate side chain in peptides of known crystal structure, which will be reported separately.

Acknowledgment. This work was supported by Columbia University New Professor Start-up Funds and a grant from the International Human Frontiers Science Program. The authors would like to thank Mr. John Williams for technical assistance.

(9) Asakawa, N.; Kurochi, S.; Kurosu, H.; Ando, I.; Shoji, A.; Ozaki, T. *J. Am. Chem. Soc.* **1992**, *114*, 3261–3265.